Inorganica Chimica Acta 368 (2011) 111–123

Contents lists available at ScienceDirect

Inorganica Chimica Acta

journal homepage: www.elsevier.com/locate/ica

Synthesis and molecular structure of the *all-trans*- and the *trans–cis*-isomers of dichlorodimethyltin complexes of phosphoric triamides

Khodayar Gholivand *, Sedigheh Farshadian

Department of Chemistry, Faculty of Sciences, Tarbiat Modares University, P.O. Box 14115-175, Tehran, Iran

ARTICLE INFO

Article history:
Received 21 November 2010
Received in revised form 20 December 2010
Accepted 21 December 2010
Available online 30 December 2010

Keywords:
Phosphoramidate
Diorganotin compounds
NMR spectroscopy
X-ray structures
Hydrogen bond
Isomers

ABSTRACT

Four new phosphoramidates with formula 4-$RC_6H_4C(O)NHP(O)(NH(CH(CH_3)_2)_2$, R = H (**1**), OCH_3 (**2**), CH_3 (**3**), Cl (**4**) and their diorganotin(IV) complexes with formula $SnCl_2(CH_3)_2(X)_2$, X = **1** (**5**), **2** (**6**), **3** (**7**) and **4** (**8**) were synthesized and characterized by NMR, IR spectroscopy and elemental analysis. The spectroscopic properties of complexes were compared with those corresponding ligands. The molecular structures for **5**, **5**·$\mathbf{CH_3CN}$, **6**·$\mathbf{CH_3CN}$, **7** and **8** were established by X-ray diffraction analysis and shown that the tin atoms have a distorted octahedral coordination with *trans*-methyl groups. Two different *all-trans* and *cis–trans* isomers were obtained by changing the crystallization solvent system. The existence of CH_3CN in molecular packing of *trans–cis* isomers might be a packing factor governing the orientation of the ligands. Due to the presence of several hydrogen bond donors and acceptors on compounds, extended hydrogen-bonded networks were observed. The structure of **2** was also determined and possesses two crystallographically independent molecules in asymmetric unit. On forming complex **6**·$\mathbf{CH_3CN}$, the ligand **2** shows shortening of C=O and P–N bond distances and increasing of P=O bond length. Pseudopolymorphism of diorganotins in **5** and **5**·$\mathbf{CH_3CN}$ is reported for the first time.

1. Introduction

Organotin(IV) compounds have been demonstrated to exhibit wide biological activity [1–3]. Insofar as many phosphoryl ligands are also noteworthy for the same reasons [4–6], a combination of the two chemistries is an interesting line to pursue. Some of these complexes have shown antitumor activity [7,8].

It has been shown that tin(IV) halide forms octahedral complexes with phosphoryl ligands of the type $R_1R_2R_3P{=}O$ having the general formula $SnX_4{\cdot}2L$ [9–14] and two isomers, with the ligand L in *cis* or *trans* mutual orientations, are possible. The strength of the Lewis basicity of the ligand, steric factors, solvent polarity and temperature may be held responsible for the differences observed [15–18]. Also, different isomers of octahedral diorganotin, $[Me_2N(CH_2)_3]_2SnF_2{\cdot}2H_2O$ were observed in solution, although X-ray diffraction analysis showed only the *all-trans*-configurated octahedral in the solid state [19].

Besides, carbacylamidophosphate and carbamoylmethylphosphine oxide derivatives, which have –C(O)XP(O)– in their molecular core units (X = NH and CH_2, respectively) are potential bidentate O,O-donor chelating ligands for metal ions, particularly for lanthanides [20–22]. However, our previous studies on carbacylamidophosphates [23–25] and Pannell studies on carbamoylmethylphosphine oxide [26] showed that they usually form dimethyltin dichloride complexes through the more basic P=O moiety. Also the products of the reactions of carbacylamidophosphates with $SnCl_2Me_2$ in 2:1 molar ratio were characterized by X-ray structure analysis and the results were *all-trans* octahedral complexes due to the fewer steric hindrance in the *trans* geometry. To our knowledge, no crystal structure of *trans–cis*-octahedral diorganotin phosphoramidate has been published yet in the literature, moreover only one paper reported crystallographically the *all-trans* and *trans–cis* isomerism in octahedral diorganotin(1V) dihalide complexes by solving the X-ray crystal structure of both isomers [27].

On the other hand, the equimolar reaction between a carbamoylmethylphosphine oxide and $SnCl_2Me_2$ led to the formation of five coordinate tin atoms with distorted trigonal bipyramidal geometry, so the reagent ratio perhaps could influence the formation of 1:1 and 2:1 complexes.

To continue our study in this field and in order to investigate the effect of reagent ratio and choice of solvent on the coordination patterns of phosphoramidate diorganotin complexes four new carbacylamidophosphates with formula 4-$RC_6H_4C(O)NHP(O)(NH(CH(CH_3)_2)_2$, R = H (**1**), OCH_3 (**2**), CH_3 (**3**) and Cl (**4**) have been synthesized. The ligands were reacted with $SnCl_2Me_2$ in 1:1 and 2:1 molar ratios in two different solvents, acetonitrile and toluene, and diorganotin complexes **5**–**8** were formed. The complexes were crystallized in various solvents and depending

* Corresponding author. Tel.: +98 2182884422; fax: +98 2182883455.
E-mail address: gholi_kh@modares.ac.ir (K. Gholivand).

0020-1693/$ - see front matter © 2010 Elsevier B.V. All rights reserved.
doi:10.1016/j.ica.2010.12.060

on the solvent, two different *all-trans* and *trans–cis*-octahedral isomers were obtained. In addition to the molecular structure of complexes, their crystal packings revealing supramolecular self assembly were also reported. The crystal structure of **2** was characterized and the bond lengths and angles were compared to those related diorganotin complex (**6·CH$_3$CN**).

2. Experimental

2.1. Materials and methods

All the chemicals used are commercially available and were used as received without further purification. ^{1}H, ^{13}C, ^{31}P and ^{119}Sn NMR specra were recorded on a Bruker Avance DRS 500 spectrometer at 500.13, 125.77, 202.46 and 186.50 MHz, respectively. ^{1}H and ^{13}C chemical shifts were determined relative to TMS. ^{31}P and ^{119}Sn chemical shifts were measured relative to 85% H_3PO_4 and $Sn(CH_3)_4$ as external standards, respectively. Infrared (IR) spectra were recorded on a Shimadzu model IR-60 spectrometer. Elemental analysis was performed using a Heraeus CHN-O-RAPID apparatus. Melting points were obtained with an Electrothermal instrument.

2.2. Synthesis of ligands

4-RC$_6$H$_4$C(O)NHP(O)Cl$_2$ (R = H, OMe, Me and Cl) were synthesized and purified using reported method [28].

Compounds **1–4** were synthesized from the reaction of 4-RC$_6$H$_4$C(O)NHP(O)Cl$_2$ (R = H, OCH$_3$, CH$_3$ and Cl, respectively) with isopropylamine in 1:4 molar ratio. The amine was added drop wise to a CH$_3$CN solution (30 ml) of 4-RC$_6$H$_4$C(O)NHP(O)Cl$_2$ and stirred at −1 °C. After 5 h, the products were filtered off and then washed with distilled water and dried.

Physical and spectroscopic data of the compounds **1–4** are presented below:

2.2.1. N-(benzoyl)-N′,N″-bis(isopropyl) phosphoric triamide (*1*)

Yield: 80%. M.p. 196-198 °C. *Anal.* Calc. for $C_{13}H_{22}N_3O_2P$ (283.31): C, 55.11; H, 7.83; N, 14.83. Found: C, 55.13; H, 7.80; N, 14.78%. IR (KBr): ν = 3270 (s), 2965(m), 1646 (s, C=O), 1492 (w), 1454 (s), 1378 (s), 1264 (w), 1206 (s, P=O), 1167 (w), 1134 (m), 1031 (m), 899 (m), 831 (w), 788 (w), 706 (m), 572 (w), 530 (w) cm^{-1}. ^{1}H NMR (CDCl$_3$): δ = 1.11 (d, $^3J_{HH}$ = 6.4 Hz, 6H, CH$_3$), 1.18 (d, $^3J_{HH}$ = 6.4 Hz, 6H, CH$_3$), 3.04 (dd, $^2J_{PH}$ = 8.7 Hz, 2H, NH$_{amine}$), 3.53 (m, 2H, CH), 7.44 (dd, $^3J_{HH}$ = 7.5 Hz, $^3J_{HH}$ = 7.9 Hz, 2H, *m*-Ph), 7.54 (t, $^3J_{HH}$ = 7.3 Hz, 1H, *p*-Ph), 7.99 (d, $^3J_{HH}$ = 7.3 Hz, 2H, *o*-Ph), 8.80 (d, $^2J_{PH}$ = 5.8 Hz, 1H, NH$_{amide}$) ppm. ^{13}C NMR (CDCl$_3$): δ = 25.22 (d, $^3J_{PC}$ = 4.8 Hz, CH$_3$), 25.63 (d, $^3J_{PC}$ = 6.9 Hz, CH$_3$), 43.33 (s, CH), 127.87 (s, C$_{ortho}$), 128.57 (s, C$_{meta}$), 132.47 (s, C$_{para}$), 133.27 (d, $^3J_{PC}$ = 7.5 Hz, C$_{ipso}$), 169.05 (s, C=O) ppm. ^{31}P NMR (CDCl$_3$,): δ = 7.49 (m) ppm.

2.2.2. N-(4-methoxy benzoyl)-N′,N″-bis(isopropyl) phosphoric triamide (*2*)

Yield: 74%. M.p. 176–178 °C. *Anal.* Calc. for $C_{14}H_{24}N_3O_3P$ (313.33): C, 53.67; H, 7.72; N, 13.41. Found: C, 53.71; H, 7.65; N, 13.45%. IR (KBr): ν = 3300 (m), 3120 (m), 2940 (m), 1634 (s, C=O), 1597 (s), 1509 (w), 1425 (s), 1311 (m), 1256 (s), 1210 (s, P=O), 1173 (s), 1133 (m), 1028 (s), 1005 (m), 896 (m), 835 (m), 775 (w), 687 (w), 541 (w), 498 (w) cm^{-1}. ^{1}H NMR (CDCl$_3$): δ = 1.10 (d, 6H, $^3J_{HH}$ = 6.4 Hz, CH$_3$), 1.17 (d, $^3J_{HH}$ = 6.4 Hz, 6H, CH$_3$), 3.10 (dd, $^2J_{PH}$ = 8.4 Hz, 2H, NH$_{amine}$), 3.53 (m, 2H, CH), 3.84 (s, 3H, OCH$_3$), 6.90(d, $^3J_{HH}$ = 8.8 Hz, 2H, *m*-Ph), 8.08 (d, $^3J_{HH}$ = 8.8 Hz, 2H, *o*-Ph), 9.43 (d, $^2J_{PH}$ = 5.8 Hz, 1H, NH$_{amide}$) ppm. ^{13}C NMR (CDCl$_3$): δ = 24.67 (d, $^3J_{PC}$ = 4.8 Hz, CH$_3$), 25.09 (d, $^3J_{PC}$ = 6.9 Hz, CH$_3$), 42.73 (s, CH), 54.83 (s, OCH$_3$), 113.09 (s, C$_{meta}$), 125.24 (d, $^3J_{PC}$ = 8.2 Hz, C$_{ipso}$), 129.77 (s, C$_{ortho}$), 162.42 (s, C$_{para}$), 168.38 (s, C=O) ppm. ^{31}P NMR (CDCl$_3$): δ = 7.47 (m) ppm.

2.2.3. N-(4-methyl benzoyl)-N′,N″-bis(isopropyl) phosphoric triamide (*3*)

Yield: 70 %. M.p. 186–188 °C. *Anal.* Calc. for $C_{14}H_{24}N_3O_2P$ (297.34): C, 56.55; H, 8.13; N, 14.33. Found: C, 56.50; H, 8.19; N, 14.35%. IR (KBr): ν = 3270 (s), 2965 (m), 1646 (s, C=O), 1611 (w), 1511 (w), 1424 (s), 1266 (w), 1208 (s, P=O), 1131 (m), 1032 (m), 898 (m), 837 (w), 799 (w), 756 (w), 572 (w), 532 (w) cm^{-1}. ^{1}H NMR (CDCl$_3$): δ = 1.13 (d, $^3J_{HH}$ = 6.4 Hz, 6H, CH$_3$), 1.20 (d, $^3J_{HH}$ = 6.4 Hz, 6H, CH$_3$), 2.41 (s, 3H, CH$_3$-Ph), 3.02 (dd, $^2J_{PH}$ = 8.4 Hz, 2H, NH$_{amine}$), 3.56 (m, 2H, CH), 7.26 (d, $^3J_{HH}$ = 7.6 Hz, 2H, *m*-Ph), 7.83 (d, $^3J_{HH}$ = 8.1 Hz, 2H, *o*-Ph), 8.19 (d, $^2J_{PH}$ = 4.7 Hz, 1H, NH$_{amide}$) ppm.·^{13}C NMR (CDCl$_3$): δ = 21.50 (s, *p*-CH$_3$), 25.27 (d, $^3J_{PC}$ = 4.7 Hz, CH$_3$), 25.67 (d, $^3J_{PC}$ = 6.9 Hz, CH$_3$), 43.38(s, CH), 127.78 (s, C$_{ortho}$), 129.38 (s, C$_{meta}$), 130.52 (d, $^3J_{PC}$ = 7.7 Hz, C$_{ipso}$), 143.28(s, C$_{para}$), 168.81 (s, C=O) ppm. ^{31}P NMR (CDCl$_3$): δ = 6.95 (m) ppm.

2.2.4. N-(4-chlorobenzoyl)-N′,N″-bis(isopropyl) phosphoric triamide (*4*)

Yield: 72%. M.p. 183–185 °C. *Anal.* Calc. for $C_{13}H_{21}ClN_3O_2P$ (317.76): C, 49.14; H, 6.66; N, 13.22. Found: C, 49.12; H, 6.70; N, 13.15%. IR (KBr): ν = 3335 (m), 3090 (w), 2970 (m), 1649 (s, C=O), 1592 (w), 1494 (w), 1449 (s), 1288 (w), 1215 (s, P=O), 1169 (w), 1132 (m), 1080 (w), 1040 (m), 1013 (m), 899 (m), 831 (w), 752 (m), 717 (w), 533 (m) cm^{-1}. ^{1}H NMR (CDCl$_3$), δ = 1.11 (d, ^3J = 6.4 Hz, 6H, CH$_3$), 1.19 (d, ^3J = 6.4 Hz, 6H, CH$_3$), 3.05 (dd, $^2J_{PH}$ = 8.1 Hz, 2H, NH$_{amine}$), 3.51 (m, 2H, CH), 7.41(dd, $^3J_{HH}$ = 8.4 Hz, $^6J_{PH}$ = 1.2 Hz, 2H, *m*-Ph), 8.08 (dd, $^3J_{HH}$ = 8.4 Hz, $^5J_{PH}$ = 1.85 Hz, 2H, *o*-Ph), 9.67 (br, 1H, NH$_{amide}$) ppm. ^{13}C NMR (CDCl$_3$): δ = 25.22 (d, $^3J_{PC}$ = 4.9 Hz, CH$_3$), 25.63 (d, $^3J_{PC}$ = 6.8 Hz, CH$_3$), 43.40 (s, CH), 128.71 (s, C$_{meta}$), 129.78 (d, $^4J_{PC}$ = 5.4 Hz, C$_{ortho}$), 131.78 (d, $^3J_{PC}$ = 8.2 Hz, C$_{ipso}$), 138.82 (s, C$_{para}$), 168.36 (d, $^2J_{PC}$ = 6.3 Hz) ppm. ^{31}P NMR (CDCl$_3$): δ = 7.41 (m) ppm.

2.3. Synthesis of complexes

Method A: one equivalent dimethyltin dichloride was added to an acetonitrile solution of one equivalent of ligand and stirred at room temperature. After 2 days, the solvent was allowed to evaporate slowly.

Method B: to a stirred solution of one equivalent of ligand, a solution of one equivalent $(CH_3)_2SnCl_2$ in toluene was added and heated (50–60 °C) for 2 h and the resulting mixture was then stirred at room temperature. After 2 days, the mixture was filtered and the resulting solution was evaporated.

Above reactions were also carried out in 2:1 molar ratio of ligands/$SnCl_2Me_2$ and the same products were obtained.

2.3.1. Bis(N-benzoyl, N′,N″-bis(isopropyl) phosphoric triamide) dimethyl stannate(IV) dichloride (*5*)

This compound was obtained by the reaction of **1** with $SnCl_2Me_2$. Yield: 52%. M.p. 170–172 °C. *Anal.* Calc. for $C_{28}H_{50}Cl_2N_6O_4P_2Sn$ (786.27): C, 42.77; H, 6.41; N, 10.69. Found: C, 42.74; H, 6.49; N, 10.75%. IR (KBr): ν = 3425 (w), 3282 (m), 2970 (w), 1669 (s, C=O), 1597 (w), 1500 (w), 1451 (s), 1426 (s), 1306 (w), 1257 (m), 1163 (s, P=O), 1151 (s), 1129 (s), 1056 (m), 1022 (m), 903 (m), 839 (m), 797 (m), 711 (m), 626 (w), 544 (m) cm^{-1}. ^{1}H NMR (CDCl$_3$): δ = 1.15 (d, $^3J_{HH}$ = 6.4 Hz, 12H, CH$_3$), 1.21 (d, $^3J_{HH}$ = 6.4 Hz, 12H, CH$_3$), 1.31 (s, $^2J(^{119}Sn, ^1H)$ = 88.6 Hz, 6H, Sn(CH$_3$)$_2$), 3.06 (dd, $^2J_{PH}$ = 9.3 Hz, 4H, NH$_{amine}$), 3.53 (m, 4H, CH), 7.48 (dd, $^3J_{HH}$ = 7.6 Hz, $^3J_{HH}$ = 7.9 Hz, 4H, *m*-Ph), 7.58 (t, $^3J_{HH}$ = 7.3 Hz, 2H, *p*-Ph), 7.98 (d, $^3J_{HH}$ = 7.5 Hz, 4H, *o*-Ph), 8.98 (br, 2H, NH$_{amide}$) ppm. ^{13}C NMR (CDCl$_3$): δ = 25.20 (d, $^3J_{PC}$ = 4.6 Hz,

CH_3), 25.57 (d, $^3J_{PC}$ = 6.9 Hz, CH_3), 43.68 (s, CH), 127.87 (s, C_{ortho}), 128.83 (s, C_{meta}), 132.38 (d, $^3J_{PC}$ = 7.9 Hz, C_{ipso}), 133.05 (s, C_{para}), 168.90 (s, C=O) ppm. ^{31}P NMR ($CDCl_3$): δ = 5.98 (m) ppm. ^{119}Sn NMR (DMSO-d_6): −238.25 ppm.

2.3.2. Bis(N-(4-methoxybenzoyl), N',N''-bis(isopropyl) phosphoric triamide) dimethyl stannate(IV) dichloride (**6**)

This compound was obtained by the reaction of **2** with $SnCl_2Me_2$. Yield: 45%. M.p. 157–159 °C. *Anal.* Calc. for $C_{30}H_{54}Cl_2N_6O_6P_2Sn$(846.32): C, 42.58; H, 6.44; N, 9.92. Found: C, 42.52; H, 6.54; N, 9.95%. IR (KBr): ν = 3400 (w), 3280 (m), 3000 (m), 1661 (s, C=O), 1603 (s), 1572 (w), 1515 (w), 1435 (s), 1406 (s), 1306 (w), 1253 (s), 1187 (m), 1161 (s, P=O), 1126 (s), 1092 (m), 1034 (s), 902 (m), 845 (m), 790 (w), 766 (w), 576 (w), 510 (w) cm^{-1}. ^{1}H NMR ($CDCl_3$): δ = 1.15 (d, $^3J_{HH}$ = 6.4 Hz, 12H, CH_3), 1.20 (d, $^3J_{HH}$ = 6.4 Hz, 12H, CH_3), 1.29 (s, 6H, ^2J(^{119}Sn, ^{1}H) = 88.9 Hz, $Sn(CH_3)_2$), 3.06 (br, 4H, NH), 3.53 (m, 4H, CH), 3.87 (s, 6H, OCH_3), 6.95 (d, $^3J_{HH}$ = 7.3 Hz, 4H, *m*-Ph), 7.94 (d, ^3J = 8.3 Hz, 4H, *o*-Ph), 8.41 (br, 2H, NH_{amide}) ppm. ^{13}C NMR ($CDCl_3$): δ = 20.90(s), 25.19 (d, $^3J_{PC}$ = 4.6 Hz, CH_3), 25.54 (d, $^3J_{PC}$ = 7.1 Hz, CH_3), 43.70 (s, CH), 55.52 (s, OCH_3), 114.09 (s, C_{meta}), 124.80 (s, C_{ortho}), 129.95 (d, $^3J_{PC}$ = 9.9 Hz, C_{ipso}), 163.48 (s, C_{para}), 168.33 (s, C=O) ppm. ^{31}P NMR ($CDCl_3$): δ = 6.18 (m) ppm. ^{119}Sn NMR (DMSO-d_6): −237.03 ppm.

2.3.3. Bis(N-(4-methylbenzoyl), N',N''-bis(isopropyl) phosphoric triamide) dimethyl stannate(IV) dichloride (**7**)

This compound was obtained by the reaction of **3** with $SnCl_2Me_2$. Yield: 44%. M.p. 159–161 °C. *Anal.* Calc. for $C_{30}H_{54}Cl_2N_6O_4P_2Sn$ (814.32): C, 44.25; H, 6.68; N, 10.32. Found: C, 44.23; H, 6.60; N, 10.35%. IR (KBr): ν = 3390 (m), 3285 (s), 2975 (m), 1673 (s, C=O), 1610 (m), 1515 (w), 1436 (s), 1366 (w), 1302 (w), 1253 (w), 1159 (s, P=O), 1124 (s), 1094 (m), 1045 (s), 902 (m), 840 (m), 791 (w), 750 (m), 573 (w), 510 (m) cm^{-1}. ^{1}H NMR ($CDCl_3$): δ = 1.15 (d, $^3J_{HH}$ = 6.4 Hz, 12H, CH_3), 1.20 (d, $^3J_{HH}$ = 6.4 Hz, 12H, CH_3), 1.33 (s, ^2J(^{119}Sn, ^{1}H) = 87.6 Hz, 6H, $Sn(CH_3)_2$), 2.42 (s, 6H, CH_3-Ph), 3.10 (dd, $^2J_{PH}$ = 9.5 Hz, 4H, NH_{amine}), 3.50 (m, 4H, CH), 7.26 (d, $^3J_{HH}$ = .7.8 Hz, 4H, *m*-Ph), 7.87 (d, $^3J_{HH}$ = 8.1 Hz, 4H, *o*-Ph), 8.83 (d, $^2J_{PH}$ = 5.8 Hz, 2H, NH_{amide}) ppm. ^{13}C NMR ($CDCl_3$): δ = 20.96(s), 21.54 (s), 25.17 (d, $^3J_{PC}$ = 4.6 Hz, CH_3), 25.52 (d, $^3J_{PC}$ = 7.0 Hz, CH_3), 43.69 (s, CH), 128.12 (s, C_{ortho}), 129.79 (d, $^3J_{PC}$ = 7.8, C_{ipso}), 143.66 (s, C_{para}), 169.02 (s, C=O) ppm. ^{31}P NMR ($CDCl_3$): δ = 5.70 (m) ppm.

2.3.4. Bis(N-(4-chlorobenzoyl), N',N''-bis(isopropyl) phosphoric triamide) dimethyl stannate(IV) dichloride (**8**)

This compound was obtained by the reaction of **4** with $SnCl_2Me_2$. Yield: 53%. M.p. 162–164 °C. $C_{28}H_{48}Cl_4N_6O_4P_2Sn$ (855.15): *Anal.* Calc. for $C_{28}H_{48}Cl_4N_6O_4P_2Sn$ (855.15): C, 39.33; H, 5.66; N, 9.83. Found: C, 39.20; H, 5.60; N, 9.75%. IR (KBr): ν = 3380 (w), 3250 (m), 2975 (m), 1651 (s, C=O), 1594 (m), 1495 (w), 1449 (s), 1302 (w), 1260 (w), 1189 (m), 1168(s, P=O), 1125 (s), 1100 (m), 1039 (m), 1010 (m), 897 (m), 796 (m), 752 (m), 719 (w), 534 (w) cm^{-1}. ^{1}H NMR ($CDCl_3$): δ = 1.15 (d, $^3J_{HH}$ = 6.4 Hz, 12H, CH_3), 1.21 (d, $^3J_{HH}$ = 6.4 Hz, 12H, CH_3), 1.29 (s, 6H, ^2J(^{119}Sn, ^{1}H) = 87.0 Hz, $Sn(CH_3)_2$), 3.06 (dd, $^2J_{PH}$ = 9.4 Hz, 4H, NH_{amine}), 3.50 (m, 4H, CH), 7.45 (d, $^3J_{HH}$ = 7.9 Hz, 4H, *m*-Ph), 7.96 (d, $^3J_{HH}$ = 8.0 Hz, 4H, *o*-Ph), 8.88 (br, 2H, NH_{amide}) ppm. ^{13}C NMR ($CDCl_3$): δ = 14.16(s), 25.14 (d, $^3J_{PC}$ = 4.6 Hz, CH_3), 25.50 (d, $^3J_{PC}$ = 6.9 Hz, CH_3), 43.83 (s, CH), 129.12 (s, C_{ortho}), 129.51 (s, C_{meta}), 130.83 (d, $^3J_{PC}$ = 8.3 Hz, C_{ipso}), 139.56 (s, C_{para}), 167.96 (s, C=O) ppm. ^{31}P NMR ($CDCl_3$): δ = 5.62 (m) ppm.

2.4. Crystal structure determination

X-ray data of compounds **2**, **5**, **5·CH$_3$CN**, **8** were collected on a Bruker SMART 1000 CCD [29–31] and for compound **6·CH$_3$CN**, **7** on a Bruker SMART APEX2 CCD area detector [32] with graphite-monochromated Mo Ka radiation (λ = 0.71073 Å). The structures were refined with SHELXTL (for **2**, **5**, **5·CH$_3$CN**, **7**, **8**) [33–35] and SHELXL-97 [36] (for **6·CH$_3$CN**) by full-matrix least-squares on F^2. The positions of hydrogen atoms were obtained from the difference Fourier map. Crystal data and experimental details of the structure determinations for compounds **2**, **1b**, **1b·CH$_3$CN** and **2b·CH$_3$CN** are listed in Table 1 and for compounds **7** and **8** are listed in Table 2.

3. Results and discussion

3.1. Synthesis and spectral characterization

The reaction of **1** with $SnCl_2Me_2$ was first investigated. The initial aim of our investigation was to synthesize of penta and hexa coordinated tin complexes by the reaction of one and two equivalents of ligands with one equivalent $SnCl_2Me_2$, respectively. However, the resulting products were only hexa coordinated complexes. When the above reactions were carried out using different solvents, such as acetonitrile and toluene only the hexacoordinate tin complexes were isolated again irrespective of the solvent (Scheme 1).

Crystallization of the product from the reaction of **1** with $SnCl_2Me_2$ in various solvents led to different results. While crystallization from CH_3CN or toluene produced *all-trans* isomers, crystallization from a mixture of acetonitrile and *n*-hexane yielded essentially the *trans–cis* isomer, the first to be observed.

We analyzed other diorganotin derivatives containing the same ligands with different para substituents on the phenyl ring in an attempt to explain why the unexpected *trans–cis* configuration of Bis (N-4-R-benzoyl, *N',N''*-bis(isopropyl)phosphoric triamide) dimethyl stannate(IV) dichloride is the form experimentally observed. The reactions of **3** and **4** with $SnCl_2Me_2$ in different reagent ratio and solvents were attempted and crystallization in the acetonitrile solution yielded *all-trans* octahedral tin complexes. However, the reaction of **2** with $SnCl_2Me_2$ in toluene and recrystallization of the product in acetonitrile/*n*-hexane solution was resulted *trans–cis* isomer as observed in **5**.

It is important to note that the molecular packing of both *trans–cis* isomers contains molecules of CH_3CN, which might be an important packing factor governing the orientation of the ligands. Therefore the conformation of the ligands probably results mainly from packing forces. The structures of **5** and **5·CH$_3$CN** are conformational pseudopolymorphic and to the best of our knowledge these are the first pseudopolymorphs of diorganotin compounds that have been obtained until now.

The compounds **1–8** were characterized by means of IR and multinuclear NMR spectroscopy. Some spectroscopic data of organotin compounds and their corresponding ligands are listed in Table 3.

The methyl protons of the two isopropyl groups appear as two different doublets ($^3J_{HH}$ = 6.4 Hz). ^{1}H NMR spectra of free ligands show a triplet (which is actually two overlapping doublets) corresponds to the amine (isopropyl) protons at 3.00–3.10 ppm ($^2J_{PH}$ = 8.1–8.7 Hz) due to the presence of two different types of N–H protons in the molecules. This value increases comparatively from the free ligands **1–4** to complexes, which is in line with the shortening of the P–N bonds. The same results were also observed in the previous reported organotin complexes of phosphonic diamides [37,38].

Table 1
Crystal data collection and structure refinement parameters for complexes **2**, **5**, **5**·CH_3CN and **6**·CH_3CN.

Compound	**2**	**5**	**5**·CH_3CN	**6**·CH_3CN
Empirical formula	$C_{14}H_{24}N_3O_3P$	$C_{28}H_{50}Cl_2N_6O_4P_2Sn$	$C_{30}H_{53}Cl_2N_7O_4P_2Sn$	$C_{32}H_{57}Cl_2N_7O_6P_2Sn$
Formula weight	313.33	786.27	827.32	887.38
T (K)	100(2)	100(2)	100(2)	100(2)
Crystal system	triclinic	monoclinic	monoclinic	monoclinic
Space group	$P\bar{1}$	$P2_1/c$	$C2/c$	$P2_1/n$
a (Å)	8.3973(3)	18.8529(10)	12.2916(11)	10.0536(5)
b (Å)	11.8993(4)	13.0348(7)	14.3903(13)	23.9795(11)
c (Å)	17.5883(6)	15.5011(8)	22.330(2)	17.9173(8)
α (°)	96.3030(10)	90	90	90
β (°)	93.6580(10)	99.2700(10)	91.589(2)	101.2390(10)
γ (°)	106.5460(10)	90	90	90
V (Å^3)	1666.14(10)	3759.5(3)	3948.2(6)	4236.7(3)
Z	4	4	4	4
Density (Mg/m^3)	1.249	1.389	1.392	1.391
μ (mm^{-1})	0.178	0.946	0.905	0.852
F(0 0 0)	672	1624	1712	1840
Crystal size (mm)	0.13 × 0.11 × 0.08	0.35 × 0.25 × 0.08	0.27 × 0.19 × 0.16	0.45 × 0.35 × 0.25
θ (°)	1.17–27.00	1.09–29.00	1.82–30.11	1.44–28.00
Reflections collected/unique	16232/7286	59043/10001	13803/5774	46701/10218
R_{int} (%)	2.02	3.75	5.58	3.04
Completeness to θ (%)	100.0	100.0	99.0	99.8
Maximum/minimum transmission	0.989/0.980	0.922/0.792	0.865/0.801	0.810/0.701
Data/restraints/parameters	7286/0/379	10001/0/404	5774/0/219	10218/0/475
Goodness-of-fit (GOF) on F^2	1.013	1.005	0.971	1.003
Final R indices [$I > 2\sigma(I)$]	R_1 = 0.0505	R_1 = 0.0229	R_1 = 0.0447	R_1 = 0.0237
	wR_2 = 0.1352	wR_2 = 0.0499	wR_2 = 0.0778	wR_2 = 0.0547
R indices (all data)	R_1 = 0.0602	R_1 = 0.0323	R_1 = 0.0832	R_1 = 0.0310
	wR_2 = 0.1515	wR_2 = 0.0517	wR_2 = 0.0883	wR_2 = 0.0578
Largest diff. peak/hole (e Å^3)	0.822 and −0.433	0.695 and −0.601	0.613 and −0.625	0.936 and −0.415

Table 2
Crystal data collection and structure refinement parameters for complexes **7** and **8**.

Compound	**7**	**8**
Formula	$C_{30}H_{54}Cl_2N_6O_4P_2Sn$	$C_{28}H_{48}Cl_4N_6O_4P_2Sn$
Formula weight	814.32	855.15
Temperature (K)	296(2)	100(2)
Crystal system	monoclinic	monoclinic
Space group	$P2_1/c$	$P2_1/c$
a (Å)	13.4136(11)	13.1841(7)
b (Å)	9.9554(7)	9.8125(6)
c (Å)	15.6336(13)	15.5437(9)
β (°)	102.321(2)	101.8300(10)
V (Å^3)	2039.6(3)	1968.2(2)
Z	2	2
Density (Mg/m^3)	1.326	1.443
Absorption coefficient (mm^{-1})	0.874	1.041
F(0 0 0)	844	876
Crystal size (mm)	0.19 × 0.16 × 0.15	0.26 × 0.17 × 0.12
θ (°)	1.55–30	1.58–30.51
Reflections collected/unique	34653/5932)	25461/5994
R_{int} (%)	2.83	4.07)
Completeness to θ (%)	99.9	99.8
Maximum/minimum transmission	0.880/0.852	0.8853/0.7736
Data/restraints/parameters	5932/40/235	5994/0/227
Goodness-of-fit (GOF) on F^2	1.001	1.026
Final R indices [$I > 2\sigma(I)$]	0.0286	0.0265
	wR_2 = 0.0713	wR_2 = 0.0582
R indices (all data)	R_1 = 0.0405	R_1 = 0.0412
	wR_2 = 0.0804	wR_2 = 0.0629
Largest diff. peak/hole (e Å^3)	1.120 and 0.743	0.668 and −0.450

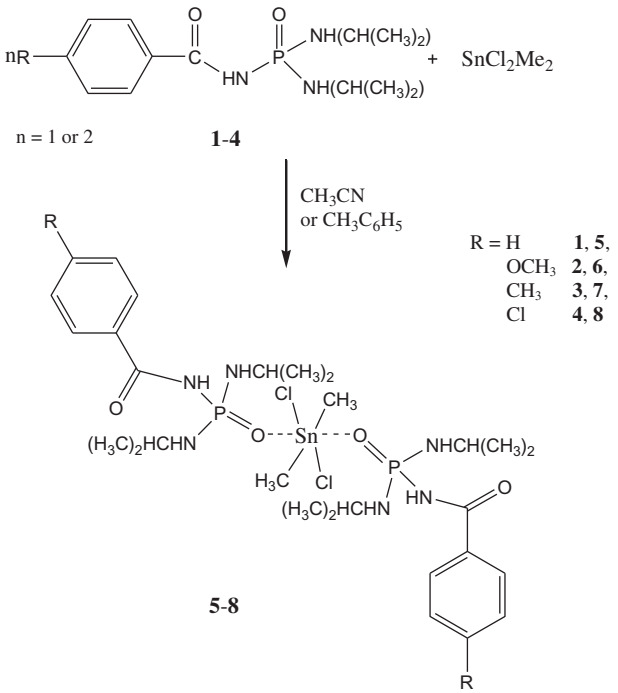

Scheme 1. Preparation pathway of diorganotin(IV) phosphoramidate **5**-**8**.

In the ^{13}C NMR spectra, two CH_3 carbons of the two isopropyl groups are not equivalent and we observe two ^3J(P,C) coupling constants in ligands and complexes. The ipso carbon atoms of phenyl rings in compounds **1**–**4** show $^3J(P,C_{aromatic})$ coupling constants in the range from 5.4 Hz (**4**) to 7.7 Hz (**3**) that increase to 7.8–9.9 Hz in complexes **5**-**8**.

As shown in Table 3, chemical shift of ^{31}P for compounds **1**–**4** are very close to each other and are in the range of 6.95–7.49 ppm. ^{31}P NMR spectra of complexes indicate that by coordinating to Sn, this parameter shows a small shift to higher fields due to disruption of the PO π interaction as a result of complex bond formation. This relatively small upfield shift (Table 3) is demonstrative of a sizeable N

Table 3
Spectroscopic NMR and IR data of the compounds.

Compound	δ^{31}P (ppm)	$^2(J_{PNH})_{amine}$ (Hz)	$^2(J_{PNH})_{amide}$ (Hz)	$^2J(^{119}SnH)$ (Hz)	$^3J(P, C_{aliphatic})$ (Hz)	$^3J(P, C_{aromatic})$ (Hz)	δ(C=O) (ppm)	ν(N–H) (cm^{-1})	ν(C=O) (cm^{-1})	ν(P=O) (cm^{-1})
1	7.49	8.7	5.8	–	4.8 6.9	7.5	169.00	3270	1646	1206
2	7.47	8.4	5.8	–	4.8 6.9	8.2	168.38	3300	1634	1210
3	6.95	8.4	4.7	–	4.7 6.9	7.7	168.81	3270	1646	1208
4	7.41	8.1	br	–	4.9 6.8	8.2	168.39	3335	1649	1215
5	5.98	9.3	br	88.6	4.6 6.9	7.9	168.90	3425	1669	1163
6	6.18	–	br	88.9	4.6 7.1	9.9	168.33	3400	1661	1161
7	5.70	9.5	5.8	87.6	4.6 7.0	7.8	169.02	3390	1673	1159
8	5.62	9.4	br	87.0	4.6 6.9	8.3	167.96	3380	1651	1168

P inductive effect by means of electron donation from the nitrogen centers to compensate the loss of electron density around phosphorus following complexation [39]. The same results have been observed in our previous studied organotin complexes with ligands of the type $RC(O)NHP(O)(R')_2$ [23–25]. However the downfield chemical shifts in comparison to that of free ligands were observed for $RP(O)(NHR')_2$ (R = alkyl, aryl) [34,35] and $((CH_3)_3CPh)_2P(O)CH_2$-$C(O)N(CH(CH_3)_2)_2$ organotin complexes [26].

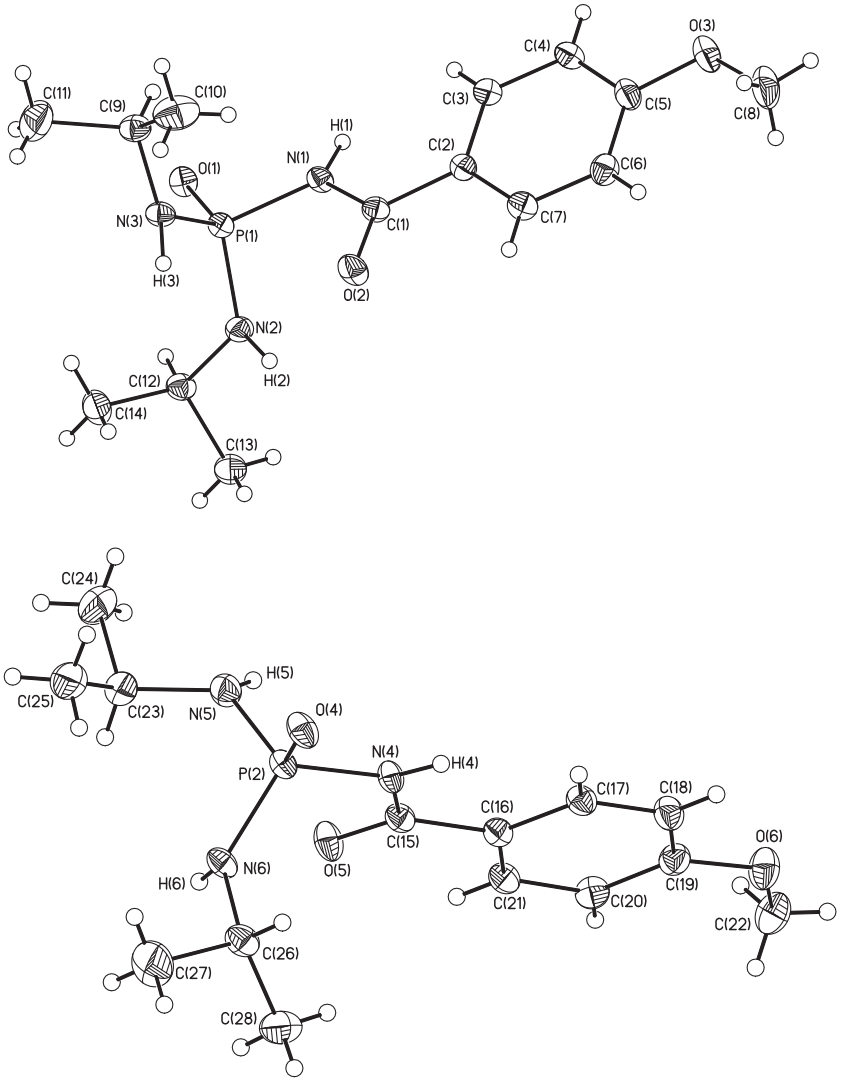

Fig. 1. Molecular structure and atom-labeling scheme for **2** (40% probability ellipsoids).

The ^{119}Sn chemical shifts of compounds **5** and **6**, at −238.25 and −237.03 ppm, respectively, are consistent with six-coordinate tin complexes [40].

In the IR spectra, the N–H stretching vibrations in ligands result in an absorption in the range of 3270–3335 cm^{-1}. In the organotin(IV) complexes this band shifts to higher energy suggesting an important influence of the coordination to tin and are consistent with the presence of different hydrogen bonding of N–H moiety in ligands (N–H···O) and complexes (N–H···Cl).

IR spectra of compounds **1**–**4** show that the ν(P=O) and ν(C=O) frequencies are in the range of 1206–1215 cm^{-1} and 1634–1649 cm^{-1}, respectively. The spectra of their organotin compounds showed a large decreasing for ν(P=O) and increasing for ν(C=O) in comparison to their related ligands. The negative significant shift of the ν(P=O) in the spectra of complexes with respect to the free ligands, is in accordance with the coordination of the phosphoryl oxygen atom to tin and confirmed by X-ray diffraction studies.

3.2. Crystal structure of 4-$CH_3OC_6H_4C(O)NHP(O)(NH(CH(CH_3)_2)_2$ (**2**)

Single crystals of **2** suitable for single crystal X-ray diffraction analysis were obtained during washing the product with distilled water. Selected structural parameters are summarized in Supplementary materials, Table S1. Compound **2** exists as two conformers in crystalline lattice. They are due to different spatial orientation of isopropyl amine groups. In one of them two amino hydrogen atoms are *syn* to the carbonyl group, but not in the other (Fig. 1).

Table 4
Hydrogen bond geometries for compound **2** [Å, °].

D–H–A	d(D–H)	d(H···A)	d(D···A)	∠DHA
N(1)–H(1)···O(4) [*x*, *y*, *z*]	0.87	1.95	2.815(2)	173
N(2)–H(2)···O(2) [*x*, *y*, *z*]	0.86	2.43	2.925(2)	117
N(3)–H(3)···O(2) [2 −*x*, −*y* + 2, −*z* + 1]	0.83	2.11	2.937(2)	174
N(4)–H(4)···O(1) [*x*, *y*, *z*]	0.88	1.98	2.844(2)	170
N(6)–H(6)···O(5) [3 −*x*, −*y* + 1, −*z*]	0.84	2.10	2.928(2)	167
C(4)–H(4A)···O(3)	0.95	2.714	3.413(2)	131.0
C(3)–H(3A)···O(4)	0.95	2.350	3.191(2)	147.2
C(22)–H(22C)···O(1)	0.98	2.554	3.495(2)	161.1
C(17)–H(17A)···O(1)	0.95	2.259	3.192(2)	167.4

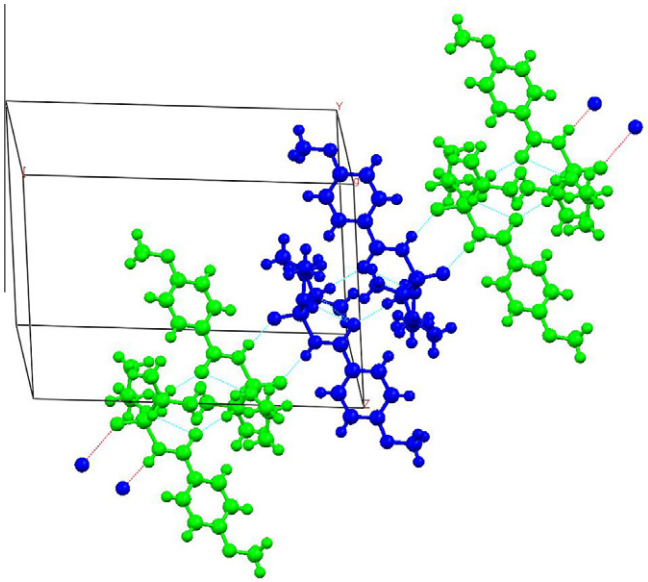

Fig. 2. View of the NH···O hydrogen bonding in the crystal structure of **2**. The two symmetry-independent forms are shown in green and blue. The dashed lines represent the hydrogen bonds. (For interpretation of the references to colour in this figure legend, the reader is referred to the web version of this article.)

The difference is also described by comparison of corresponding torsion angles in two conformers. Torsion angles P(1)–N(3)–C(9)–C(10) and P(1)–N(3)–C(9)–C(11) are −114.23(16)° and 122.17(17)°, whereas P(2)–N(5)–C(23)–(C25) and P(2)–N(5)–C(23)–C(24) are 52.8(2)° and 175.62(14)°, respectively.

The sum of the surrounding angles around N(1) and N(4) are slightly lower than sp^2 angles, 357.9 and 359.3°, respectively and as usual for such species, they are nearly planar. The other nitrogen atoms in the molecules are distorted from planarity and the sum of the angles around them are in the range of 349.2–355.01°.

As expected, the P–N_{amide} bond lengths (N_{amide} is the nitrogen atom of P(O)N(H)C(O) moiety) are longer than the P–N_{amine} distances (N_{amine} is the nitrogen atom of P(O)NR moiety), because of the resonance interaction of the N_{amide} with the C=O π system that causes a partial multiple bond character in C–N_{amide} (the C–N_{amide} bond lengths are shorter than the C–N_{amine} bond lengths, Table S1). All of these P–N bonds are shorter than the typical P–N single bond length (1.77 Å) [41]. This is likely due to the electrostatic effects (polar bonds) which overlap with P–N σ bond [42].

The P=O and C=O bonds are anti and the bond lengths fall within the norms for these linkages in phosphoramidates [43,44]. The phosphorus atoms have a distorted tetrahedral configuration with angles in the range of 105.48(7)–113.93(7)° for P(1), 103.29(7)–116.68(8)° for P(2).

The hydrogen bonding data are given in Table 4. Each independent molecule is connected to its symmetrically similar molecule via two equal –C=O···H–N– hydrogen bonds and produces a centrosymmetric dimer in the crystal lattice. The observed hydrogen-bonding pattern is of the DA:::AD type (A = H bond acceptor and D = H bond donor). These dimeric aggregates are connected to each other via –P=O···H–N– hydrogen bonds to form a 1D polymer (Fig. 2).

Besides the strong hydrogen bonds, the packing of **2** is further stabilized by a system of weaker intermolecular C–H···O hydrogen bonds as listed in Table 4. The methoxy group of the first independent molecule acts as an acceptor H bond and is involved in CH···O interaction with hydrogen atom on a benzene of its symmetrically related molecule and vice versa, forming an eight-membered {···OCCH}2 synthon (by DA:::AD type double hydrogen bond). However, the methoxy group of the second molecule is C–H···O interaction donor for the phosphoryl group of the first molecule. Furthermore, the oxygen atoms of phosphoryl groups, O1 and O4 are involved in CH···O hydrogen bonds with hydrogen atoms on aromatic rings of the second and first molecules, respectively (Fig. 3). All the geometrical data of above CH···O interactions fall into the normal range of the CH···O hydrogen bonding [45]. The centroid-to-centroid distance between two parallel phenyl rings of the first and second molecules are 3.713 and 3.753 Å, respectively, indicating the presence of π–π stacking interactions. The CH···O H-bonding and π–π stacking interactions assemble the 1-D chains to form a 3-D supramolecular architecture.

3.3. Crystal structures of $SnCl_2(CH_3)_2[C_6H_5C(O)NHP(O)(NHCH(CH_3)_2)_2]_2$ (**5**) and $SnCl_2(CH_3)_2[C_6H_5C(O)NHP(O)(NHCH(CH_3)_2)_2]_2{\cdot}CH_3CN$ (**5**·**CH_3CN**)

Suitable single crystals for X-ray diffraction analysis of **5** and **5**·**CH_3CN** were obtained by crystallization of **5** from toluene and acetonitrile/n-hexane, respectively. The molecular structures for **5** and **5**·**CH_3CN** are shown in Figs. 4 and 5, respectively and selected bond lengths and angles are listed in Supplementary materials, Tables S2 and S3, respectively. Pseudopolymorphs **5** and **5**·**CH_3CN**

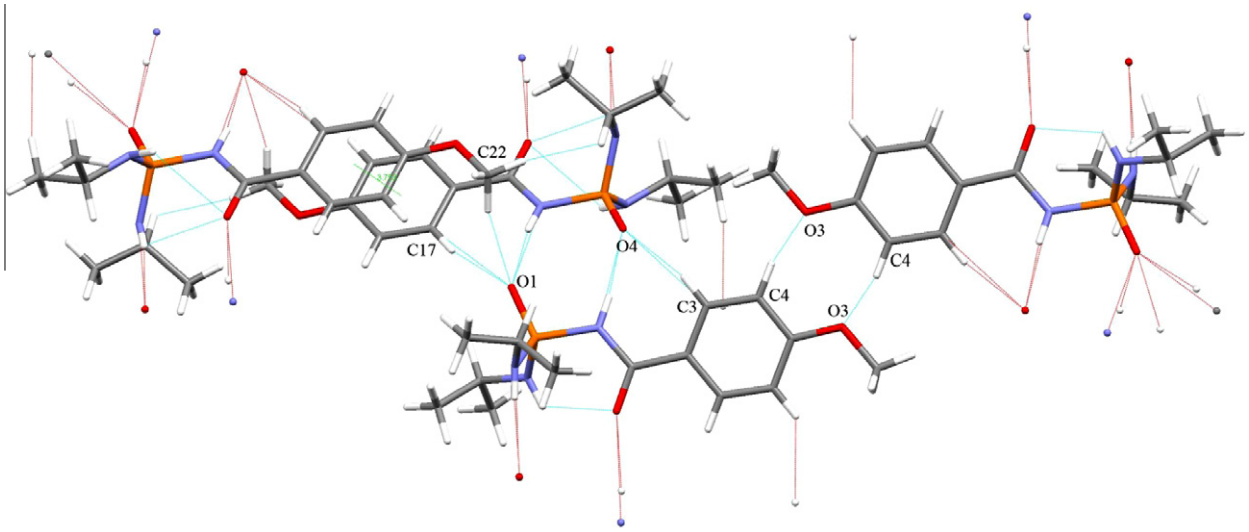

Fig. 3. Intermolecular π–π and CH···O interactions in **2**.

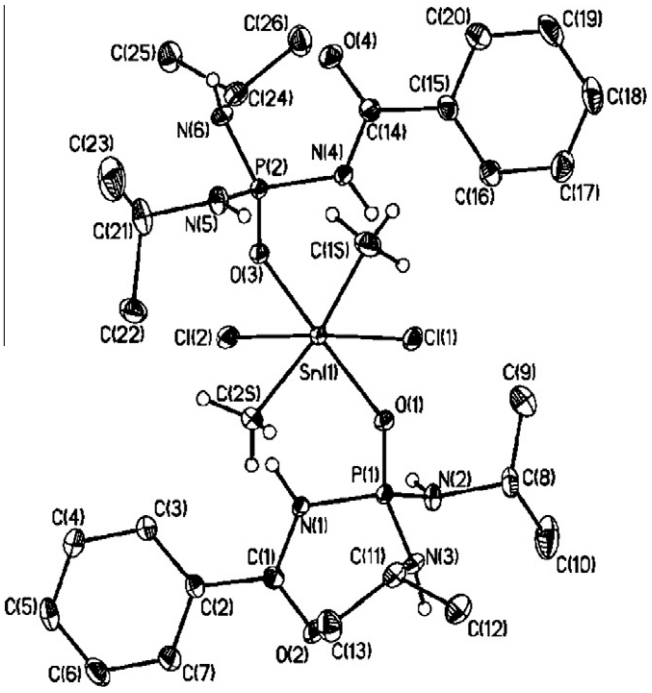

Fig. 4. Molecular structure and atom-labeling scheme for complex **5** (50% probability ellipsoids).

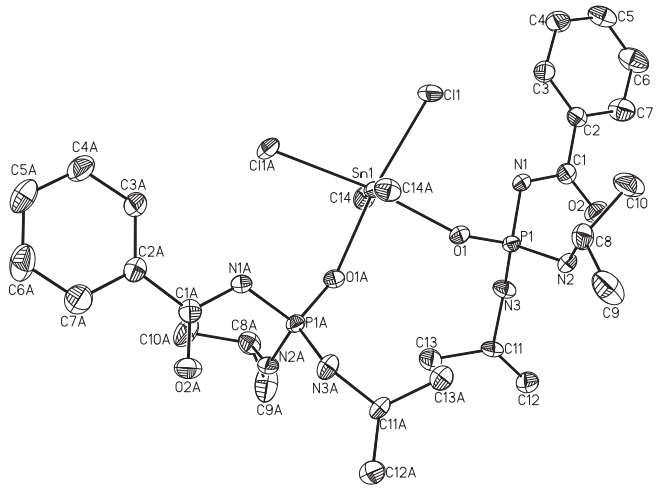

Fig. 5. Molecular structure and atom-labeling scheme for complex **5·CH$_3$CN** (50% probability ellipsoids).

crystallize in the same crystal system (monoclinic) but in different space groups ($P2_1/c$ and $C2/c$, respectively).

The tin atoms of **5** and **5·CH$_3$CN** are hexacoordinated by two carbon, two oxygen and two chlorine atoms and show distorted *all-trans* and *trans–cis* octahedral configuration, respectively. The *trans* bond angles around Sn atom of **5** are 169.82(7) [C(1S)–Sn(1)–C(2S)], 172.14 [O(1)–Sn(1)–O(3)] and 173.847(13)° [Cl(1)–Sn(1)–Cl(2)], being smaller than the ideal value of 180°. The corresponding angles (178.52(15), 177.50(6) and 177.78(6)°, respectively) that observed for the *all-trans*-$SnCl_2(CH_3)_2[C_6H_5P(O)(NHCH(CH_3)_2)_2]_2$ [38] were closer with this value. In pseudopolymorph **5.CH$_3$CN** the *trans* bond angles are 173.97° [C(14)#1–Sn(1)–C(14)] and 172.76(5)° ([O(1)#Sn(1)–Cl(1)] and [O(1)–Sn(1)–C(l)#1]). So, the deviation of C–Sn–C in **5** (10.18°) is larger than the corresponding one found for **5·CH$_3$CN** (6.03°). In our previous studied diorganotin compounds of ligands with –C(O)NHP(O)– skeleton, the trans angles around tin atoms were exactly linear (180°), the molecules were centerocymetric and the central tin atom occupied a center of inversion [23–25]. But two different Sn–O distances (2.2031(11) and 2.2224(10) Å) and also two different P–O–Sn angles (145.48(7) and 150.09(7)°) can be observed in **5**. The shorter Sn–O distance corresponds to the larger P–O–Sn angle (and reverse). These Sn–O bond lengths are a little longer than the Sn–O covalent bond [2.038–2.115 Å] [46–49]. We also note larger differences in Sn–Cl bond lengths. Thus, the Sn–Cl(2) bond is the longest at 2.7106(4) Å amongst all the Sn–Cl bonds observed in this study and those found for diorganotin compounds and is comparable with the Sn–Cl found in diorganotin compounds with bridged Cl atoms between two tin centers [50]. **5·CH$_3$CN** shows three couples of identical Sn–ligand distances. The Sn–C bond lengths [2.1075(17) and 2.1107(16) Å in **5** and 2.106(3) Å in **5·CH$_3$CN**] are consistent with those reported in other organotin(IV) complexes.

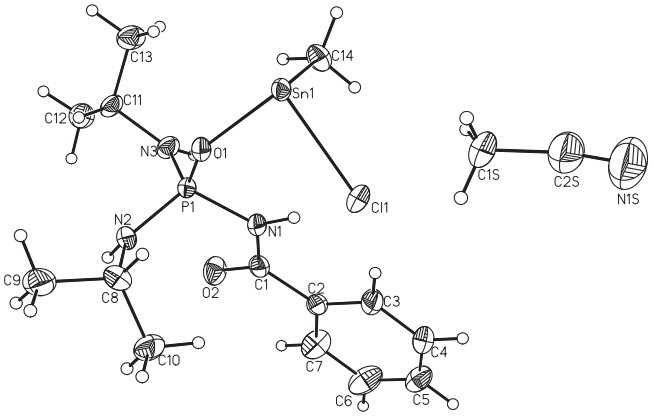

Fig. 6. Independent part of unit cell contains half of complex (located on two-fold axis) and half of acetonitrile solvent disordered over two-fold axis in **5·CH$_3$CN**.

Although the difference is not very significant, the Sn–O bonds are slightly longer in the *trans–cis* complex (2.2250(9) Å) compared to its *all-trans* indicating a greater *trans* influence of the chlorine ligands compared to the phosphoramidate ligands.

In **5** the different ligands are *cis* to each other and C–Sn–O, C–Sn–Cl and O–Sn–Cl bond angles are in the range of 84.70(5)–98.37(3)°. In **5·CH$_3$CN** the *cis* angles are in the range of 85.57(10) [C(14)–Sn(1)–O(1)#1] to 99.76(4)° [Cl(1)–Sn(1)–Cl(1)#1]. On going from the *all-trans* to the *trans–cis* isomer, no significant differences are observed in the P═O distances (1.4948(11) and 1.4971(11) Å for **5** and 1.493(2) Å for **5·CH$_3$CN**). These bond lengths are slightly shorter than the values found for $SnCl_2(CH_3)_2[C_6H_5P(O)(NHCH(CH_3)_2)_2]_2$ (1.505(2) and 1.502(2) Å) [38]. These changes presumably reflect the effect of the addition of –NHC(O)– group. As a consequence, the P–N$_{amine}$ bonds in these complexes are shorter due to increased hyperconjugation of the nitrogen lone pairs to the phosphorus atom [51]. These results are consistent with the ^{31}P NMR chemical shift differences observed between **5** and $SnCl_2(CH_3)_2[C_6H_5P(O)(NHCH(CH_3)_2)_2]_2$ [38].

The P═O distance (1.489(3) Å) in o-$C_6H_4(SnClMe_2)_2.(Me_2N)_3PO$ [50] with three P–N$_{amine}$ bonds is shorter than those of **5**–**8** due to lack of interaction between carbonyl group with nitrogen center in the former and hence better electron donation from the nitrogen center to the phosphoryl group.

Some of the carbons of isopropyl groups in **5** (C(9), C(22) and C(23)) are disordered over two positions with relative occupancies 0.6/0.4. Independent part of unit cell of **5·CH$_3$CN** contains half of complex (located on two-fold axis) and half of acetonitrile solvent disordered over two-fold axis (Fig. 6).

In all of organotin compounds **5**–**8**, each molecule has six NH bonds that two NH$_{amide}$ are involved in hydrogen bonding with the chlorine atoms of the same molecule, so two six-membered rings around tin are formed. These rings that made up six different elements coming from five different groups of the main group (group 1 (H), group 14 (Sn), group 15 (N, P), group 16 (O), group 17 (Cl)) were also observed in diorganotin phosphonic diamides [37,38] with this different that in them one of the two N–H of isopropylamines on each phosphonic diamide is involved in hydrogen bonding. Furthermore, in **5**, the three N–H$_{amine}$ participate in intermolecular hydrogen bonding with the chlorine and carbonyl groups of neighboring molecules (Table 5) and two dimensional polymeric structures were obtained parallel to the *bc* plane.

In the crystal structure, weak C–H···O [C(5)–H(5A)···O(3): d(H5A···O3) = 2.699 Å, d(C5···O3) = 3.606 Å and ∠C5–H5A···O3 = 159.98°] and C–H···Cl [C(25)–H(25B)···Cl(1): H25A···Cl1 = 2.833 Å, C25···Cl1 = 3.761 Å and ∠C25–H25B···Cl1 = 158.02°] intermolecular interactions are also found. These data are in agreement with those reported in the literature [45,52]. In addition, an intramolecular N···O short contact is observed between the oxygen of one carbonyl group and a N$_{amine}$ (d(N3···O2) = 2.945 Å).

In **5·CH$_3$CN**, hydrogen bonded chains along the *c* axis are formed by the intermolecular double N2–H2···O2 hydrogen bonds and disordered acetonitrile molecules are located in the spaces between the chains (Fig. 7). There is no hydrogen bonding between the polymer chains and acetonitrile molecules. Indeed, there are only van der Waals interactions between neighbouring chains and the solvent molecules establish only weak C–H···π interactions [d(C6···Cg) = 3.485 Å (Cg: center of CN bond), d(H6A···Cg) = 2.804 Å and ∠(C6–H6A···Cg) = 129.56°] with the host that is comparable to those found in the literature [53]. The intramolecular N···O short contacts (d(N3···O2) = 3.010 Å) is also present in the structure.

3.4. Crystal structure of $SnCl_2(CH_3)_2[p$-$CH_3OC_6H_4C(O)NHP(O)(NHCH(CH_3)_2)_2]_2$·$CH_3CN$ (**6·CH$_3$CN**)

Monoclinic crystals of **6·CH$_3$CN** were grown from a concentrated acetonitrile/n-hexane solution at room temperature. The molecular structure of complex **6·CH$_3$CN** with the atom-labeling scheme are depicted in Fig. 8 and a selection of bond lengths and angles is given in Supplementary materials, Table S4. The tin atom shows a distorted *trans*(C, C) *cis*(O, O) *cis*(Cl, Cl) octahedral configuration.

Table 5
Hydrogen bonds for compounds **5**, **5·CH$_3$CN**, **6·CH$_3$CN**, **7** and **8** [Å, °].

Compound	D–H–A	d(D–H)	d(H···A)	d(D···A)	∠DHA
5	N(1)–H(1 N)···Cl(2) [x, y, z]	0.91	2.38	3.2642(14)	165
	N(3)–H(3 N)···O(4) [x, y + 1, z]	0.91	2.13	3.0276(18)	166
	N(4)–H(4 N)···Cl(1) [x, y, z]	0.88	2.42	3.2695(14)	162
	N(5)–H(5 N)···Cl(2) [x, $-y$ + 3/2, z + 1/2]	0.86	2.77	3.6122(15)	166
	N(6)–H(6 N)···O(2) [x, y − 1, z]	0.82	2.11	2.8806(18)	157
5·CH$_3$CN	N(1)–H(1)···Cl(1) [x, y, z]	0.90	2.54	3.356(3)	151
	N(2)–H(2)···O(2) [$-x$, $-y$, $-z$ + 1]	0.90	2.10	2.994(3)	172
6·CH$_3$CN	N(6)–H(1N6)···O(2) [$-x$ − 1/2, y − 1/2, $-z$ + 3/2]	0.79	2.17	2.945(2)	168
	N(4)–H(1N4)···Cl(1) [x, y, z]	0.85	2.41	3.238(1)	166
	N(1)–H(1N1)···Cl(2) [x, y, z]	0.84	2.37	3.194(1)	165
	N(3)–H(1N3)···O(5) [$-x$ − 1/2, y + 1/2, $-z$ + 3/2]	0.80	2.21	3.001(2)	169
	N(2)–H(1N2)···O(6) [$-x$ + 1/2, y + 1/2, $-z$ + 3/2]	0.74	2.56	3.279(2)	165
	N(5)–H(1N5)···O(3) [$-x$ + 1/2, y − 1/2, $-z$ + 3/2]	0.80	2.32	3.105(2)	171
7	N(1)–H(1 N)···Cl(3) [1 − x, $-y$, $-z$]	0.87	2.45	3.2908(17)	163
	N(3)–H(3 N)···Cl(3) [2 − x, y + 1/2, z + 1/2]	0.87	2.51	3.3714(18)	171
8	N(1)–H(1)···Cl(1) [$-x$, $-y$, $-z$]	0.88	2.41	3.2568(15)	161
	N(3)–H(3)···Cl(1) [$-x$, y + 1/2, $-z$ + 1/2]	0.88	2.43	3.3114(16)	175

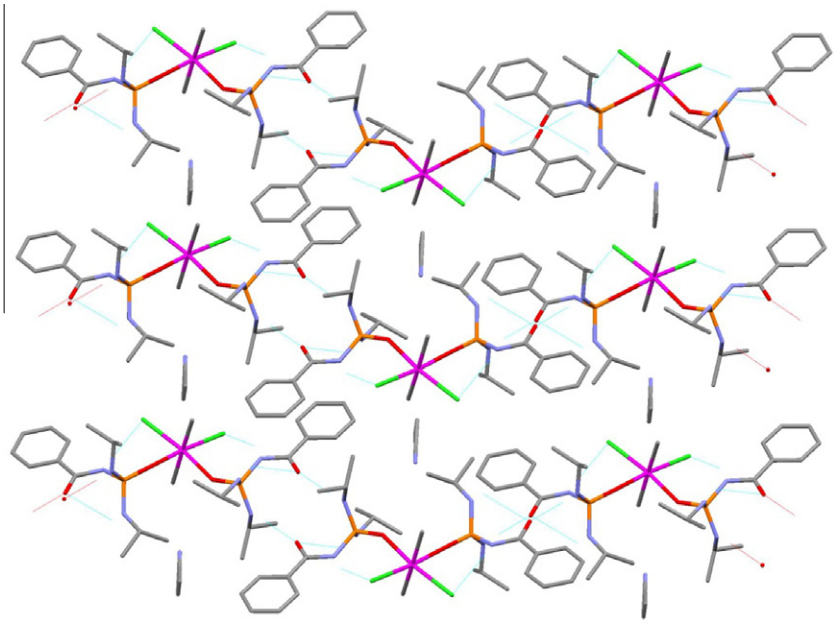

Fig. 7. View of the H-bonded chains along *c* axis produced by N2–H2···O2 H-bonds in **5·CH$_3$CN** with disordered acetonitrile molecules between chains. Hydrogen atoms are omitted for clarity.

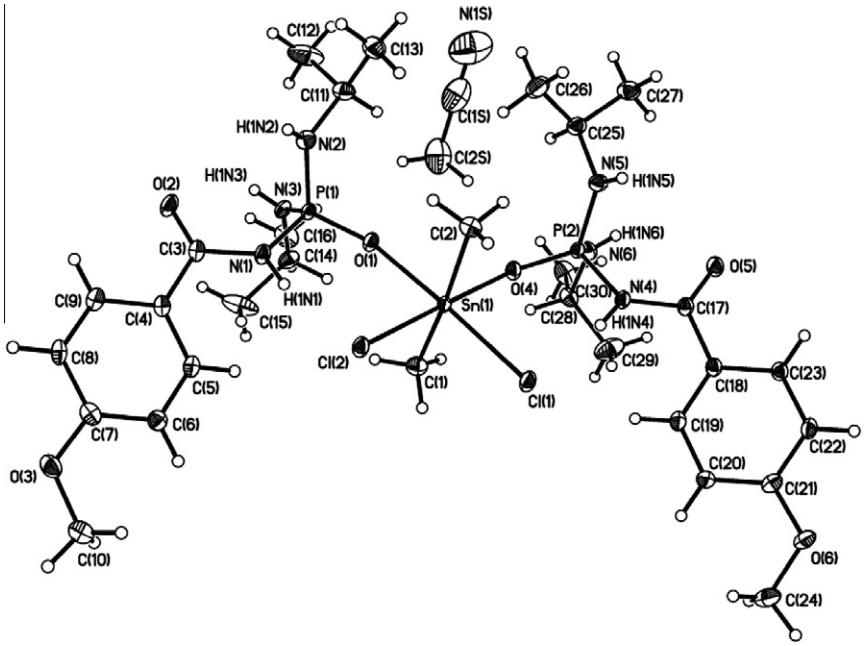

Fig. 8. Molecular structure and atom-labeling scheme for complex **6·CH$_3$CN** (50% probability ellipsoids).

In *trans* position of the two oxygen atoms are chlorines and distances are correlated: the shorter is Sn–O, the longer is Sn–Cl (perhaps '*trans* effect'). In this complex in spite of **5** the longer Sn–O distance corresponds to the larger P–O–Sn angle.

The bond angles O–Sn–Cl (177.44(3) and 179.19°) deviate slightly from the idealized value, 180°, and the deviation is smaller than the corresponding one found for **5·CH$_3$CN**. On the other hand the O–Sn–O bond angle 90.97(4)° is closer to 90° than one in **5·CH$_3$CN**, 99.79(4)°. In fact the smallest bond angles for the couples of *cis* atoms is that relevant to the C(1)–Sn(1)–O(1) angle (84.43(6)°); whereas the largest value is, that for C(2)–Sn(1)–Cl(1) (93.87(5)°).

The O–Sn–O–P torsion angles found are O(1)–Sn(1)–O(1)–P(1) = 121.1(2)° for **5·CH$_3$CN,** O(1)–Sn(1)–O(4)–P(2) = 136.83(11)° and O(4)–Sn(1)–O(1)–P(1) = −164.71(14)° for **6·CH$_3$CN**. This indicates the more coplanar arrangement of the ligand with the tin atom in **6·CH$_3$CN** than **5·CH$_3$CN**. The O–P···P–O torsion angle is 29.26° in **6·CH$_3$CN**, 96.29° in **5·CH$_3$CN** and 162.19° in **5**.

The bond angles around phosphorus P1 (in the range from 105.47(8) to 116.26(7)°) and P2 (104.92–118.26°) indicate distorted tetrahedral geometry, with the larger values displayed by the O–P–N angles (Table S4). The P═O bond lengths in this molecule (1.4951(11) and 1.4993(12) Å) are longer than the normal P═O bond length (1.45 Å) [41] and that of the corresponding

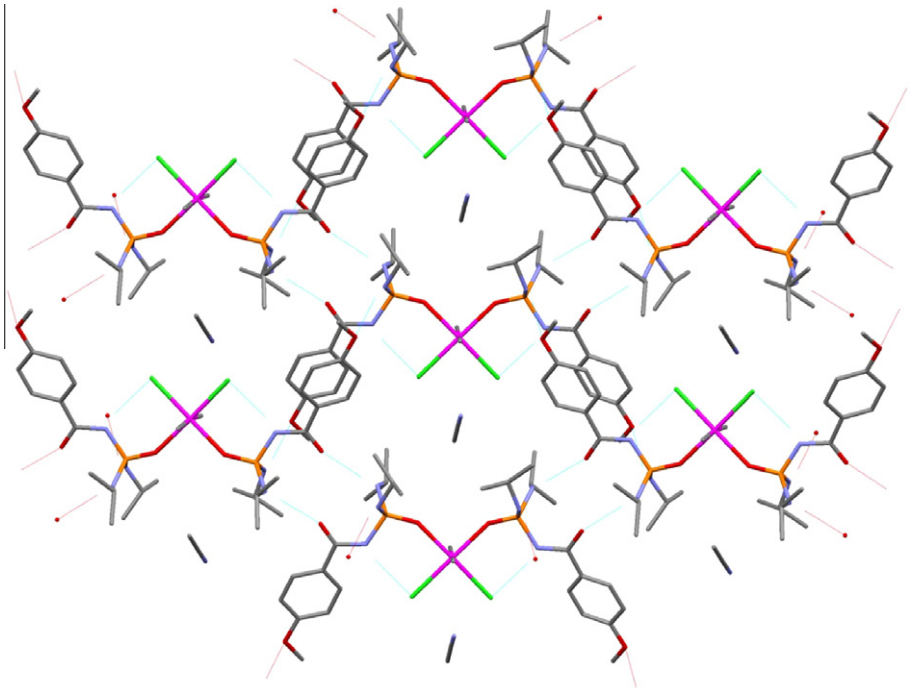

Fig. 9. 2D hydrogen bonded layered network in **6·CH$_3$CN** in the *ab* plane. (The H atoms were omitted for clarity).

ligand, **2**. This lengthening is consistent with the low stretching frequency observed in the IR spectra may also explain the differences observed in the ^{31}P NMR chemical shifts between the free and bound ligands in solution.

On forming complex **6·CH$_3$CN**, the ligand **2** also shows shortening of C=O and P–N bond distances. The C=O bond lengths decrease from 1.234(2) in **2** to 1.224(2) and 1.2185(19) in **6·CH$_3$CN**. The P–N$_{amide}$ bonds decrease from 1.6946 (14) and 1.6951(14) Å in **2** to 1.6745(14) and 1.6756 (14) Å in **6·CH$_3$CN**. Also, the P–N$_{amine}$ bond lengths decrease from 1.6243(13)–1.6470(16) Å to 1.6108(14)–1.6207(14) Å. These observations represent the increasing of the P–N bond order as observed in our previous phosphoramidate complexes [54]. The carbon–nitrogen bond adjacent to the carbonyl group (N1–C1 and N4–C17) with internuclear distances of 1.379(2) and 1.383(2) Å is considerably longer than the bond lengths in ligand (1.365(2) Å).

The asymmetric unit of compound **6·CH$_3$CN** contains one complex and one CH$_3$CN molecule. The main axis of the N(1S)–C(2S)–C(1S) acetonitrile molecule in **5·CH$_3$CN** is coplanar with the C–Sn–C plane and is nearly perpendicular to the plane of the Cl(1)Cl(1A)O(1)O(1A), the CH$_3$ group being directed towards the inside. However in **6·CH$_3$CN** the angles of this axis with C–Sn–C and the plane of Cl(1)Cl(2)O(1)O(4) are 78.75 and 57.16°, respectively.

Due to the presence of hydrogen bond acceptor methoxy groups, **6·CH$_3$CN** exhibits a crystal packing, which is entirely different from that of **5·CH$_3$CN**. In **6·CH$_3$CN**, in addition to carbonyl groups, the oxygen atoms of methoxy groups also participate in intermolecular hydrogen bonds with N–H groups (Table 5), forming infinite layers parallel to the *ab* plane (Fig. 9). The centroid–centroid distance between aromatic planes in the layers is 4.133 Å, indicating no strong π–π stacking interactions exist in complex. The layer stacking forms channels along the *c* axis filled by acetonitrile molecules. The acetonitrile molecule is linked to the channel *via* a weak C(2S)–H(2SC)···Cl(2)–Sn(1) interaction [*d*(C(2S)···Cl(2) = 3.641 Å, d(H(2SC)···Cl2) = 2.905 Å and ∠C(2S)–H(2SC)···Cl(2) = 134.26°] and also the C–H···π interaction between C(25)–H(25A) and nitrile bond [*d*(C25···Cg) = 3.596 Å, *d*(H25A···Cg) = 2.893 Å and ∠C25–H25A···Cg = 129.51]. Furthermore, C–H···Cl–Sn weak interaction between C(24) of methoxy group and Cl(2) also stabilize the structure, the C(24)···Cl(2) and H(24A)···Cl(2) distances are 3.601 and 2.869 Å, respectively.

As mentioned in Section 3.3., the CH$_3$CN molecule in **5·CH$_3$CN** is disordered over two positions participating in the host–guest C–H···π bond. On the other hand, the crystal structure refinement reveals that the guest molecule in **6·CH$_3$CN** occupies one principal site and the molecule in that site participates in both C–H···π and C–H···Cl bonding, suggesting that the additional bond effectively locks each CH$_3$CN molecule on a particular site within the channel.

*3.5. Crystal structures of SnCl$_2$(CH$_3$)$_2$[p-CH$_3$C$_6$H$_4$C(O)NHP(O)(NHCH(CH$_3$)$_2$)$_2$]$_2$ (**7**) and SnCl$_2$(CH$_3$)$_2$[p-ClC$_6$H$_4$C(O)NHP(O)(NHCH(CH$_3$)$_2$)$_2$]$_2$ (**8**)*

Colorless crystals of **7** and **8** were obtained from a concentrated CH$_3$CN solution at room temperature. Figs. 10 and 11 show ORTEP representation of the molecular structure for complex **7** and **8**, respectively, and their selected bond distances and angles are listed in Supplementary materials, Table S5. These complexes are isostructural with space group $P2_1/c$ and $Z = 2$. The molecules are centrosymmetric and identical ligands are in *trans* positions with the bond angles of 180.0° around Sn atom. The different ligands are *cis* to each other and C–Sn–O, C–Sn–Cl and O–Sn–Cl bond angles do not deviate from 90° by more than 1.91° and 2.02° for **7** and **8**, respectively. The Sn–C bond lengths are 2.097(2) Å in **7** and 2.1063(18) Å in **8** that are quite close to those reported in the literature. The Sn–Cl bond lengths (2.5909(6) and 2.5922(4) Å in **7** and **8**, respectively) lying in the normal covalent radii 2.37–2.60 Å [55–57]. The Sn–O bond distances (2.2303(13) and 2.2300(11) Å) are longer than the sum of the covalent bond radii of Sn and O [46–49], but are considerably shorter than the sum of their van der Waals radii of 3.71 Å [58].

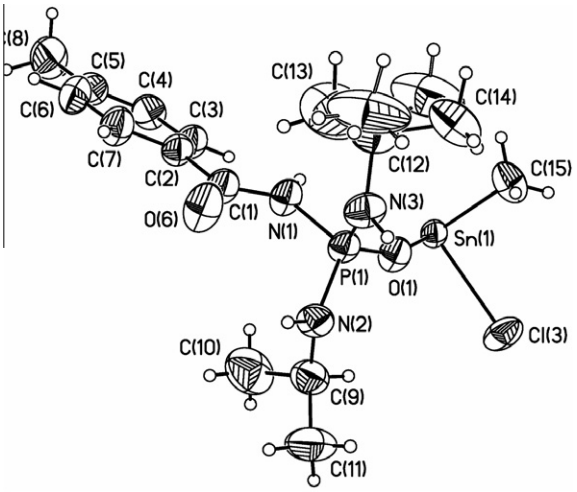

Fig. 10. The unit-cell contents for **7**. Atoms are represented by thermal ellipsoids (p = 50%). The C(13) and C(14) atoms are disordered over two positions with occupation ratio 0.6:0.4.

In the crystal structure of **7**, the carbon atoms of one of the isopropyl groups of each ligand (C(13) and C(14)) are disordered over two positions with occupation ratio 0.6:0.4. The same disorder was also observed for C(12), C(13) carbon atoms of **8**.

As a result of intermolecular N–H···Cl hydrogen bonds (Table 5) two dimensional polymeric chains are obtained in the crystal packings of **7** and **8**. Also, the carbonyl groups are involved in CH···O intermolecular hydrogen bonds as acceptors [C(4)–H(4A)···O(6) in **7**: d(C4···O6) = 3.317 Å, d(H4A···O6) = 2.465 Å and ∠(C4–H4A···O6) = 152.37°; C(4)–H(4A)···O(2) in **8**: d(C4···O2) = 3.301 Å, d(H4A···O6) = 2.407 Å and ∠(C4–H4A···O2) = 156.73°] and the para chlorine atoms of **8** participate in weak intramolecular C(8)–H(8A)···Cl(2) interactions [d(C8···Cl2) = 3.564 Å, d(H8A···Cl2) = 2.868 Å and ∠(C8–H8A···Cl2) = 128.73°]. Intermolecular C–H···Cl interactions between Cl(1) and H atoms belonging to the disordered methyl groups are also found in **8**.

3.6. Comparison of the structures for complexes **5**, **5**·CH_3CN, **6**·CH_3CN, **7** and **8**

The Sn–O bond lengths in above complexes decrease in the following order: **6**·CH_3CN > **7** ≈ **8** > **5**·CH_3CN > **5**. The smallest Sn–O bond distances for compounds **1b** and **1b**·CH_3CN is presumably due to the less steric hindrance. Interestingly, in the *all-trans* configurated diorganotins, the Sn–O distance is shorter and the Sn–Cl distance is longer (Table 6). Apparently, this is the result of both the *trans* configuration and the chlorine atoms being involved in intermolecular Cl···H–N hydrogen bonding in *all-trans* compounds. The Sn–O distances in these compounds are comparable with the Sn–O distances found in *o*-$C_6H_4(SnClMe_2)_2$.$(Me_2N)_3PO$ and ($Ph_2ClSnCH_2)_2$.$(Me_2N)_3PO$ [50,59].

The Sn–O–P angles are not linear and the *all trans*-octahedral complexes exhibit greater Sn–O–P angles than *trans–cis* ones. Among them **7** (153.83(9)°) and **8** (153.20(8)°) have the largest value. In *all-trans* isomers the tin atoms are nearly eclipsed with the N_{amidic} of the phosphoramide (torsional angle Sn–O–P–N_{amidic} 17.04(14) and -9.43(16)° in **5**, 4.7(3)° in **7** and 3.59(19)° in **8**). The corresponding torsion angles are 31.9(2)° in **5**·CH_3CN, −25.51(15) and 44.25(13)° in **6**·CH_3CN.

In these diorganotin compounds, like phosphoric triamide ligands, the C=O and P=O groups adopt anti configuration as a result of the dipole–dipole repulsion. The O–P–N–$C_{carbonyl}$ torsion

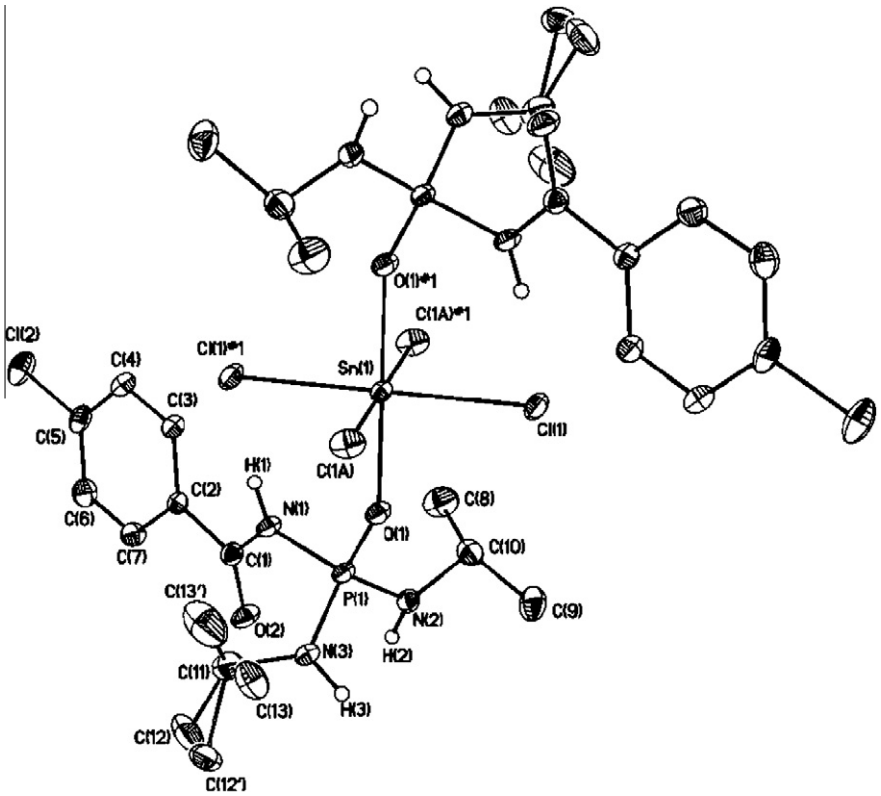

Fig. 11. Molecular structure and atom-labeling scheme for complex **8** (50% probability ellipsoids).

Table 6
Selected bond lengths (Å) angles (°) for complexes.

Compound	d(Sn–O)	d(Sn–Cl)	d(P=O)	d(P–N_{amide})	d(P–N_{amine})	d(C=O)	∠(C–Sn–C)	∠(P–Sn–O)
5	2.2031(11)	2.5244(4)	1.4948(11)	1.6840(13)	1.6163(13)	1.2217(19)	169.82(7)	145.48(7)
	2.2224(10)	2.7106(4)	1.4971(11)	1.6842(13)	1.6187(13)	1.2202(19)		150.09(7)
					1.6139(14)			
					1.6145(13)			
5·CH_3CN	2.2250(19)	2.5725(8)	1.493(2)	1.685(2)	1.611(2)	1.219(3)	173.97(18)	146.88(12)
					1.614(2)			
6·CH_3CN	2.2640(11)	2.5495(4)	1.4951(11)	1.6745(14)	1.6167(15)	1.224(2)	171.44(7)	148.85(7)
	2.2670(11)	2.5615(4)	1.4993(12)	1.6756(14)	1.6202(14)	1.2185(19)		143.23(7)
					1.6108(14)			
					1.6129(17)			
7	2.2303(13)	2.5906(6)	1.4907(15)	1.6813(16)	1.6036(19)	1.213(2)	180	153.83(9)
					1.6129(17)			
8	2.2300(11)	2.5922(4)	1.4947(12)	1.6829(14)	1.6115(15)	1.2222(2)	180	153.20(8)
					1.6202(15)			

angles are in the range −159.56(12) to 172.4(2)°. The O–C···P–O torsion angles are in the range 162.82–179.29°.

The sums of angles around nitrogen amidic in the complexes vary in the range of 359.29 –360.02° and these atoms are perfectly sp^2 hybridized. The sums of angles around other nitrogen atoms are in the range of 350.97–359.83° and some of them are pyramidal.

As observed in **2**, in these complexes P–N_{amide} bond lengths are longer than the P–N_{amine} bonds in agreement with solution data that $(^2J_{PNH})_{amine}$ is greater than $^2(J_{PNH})_{amide}$. Also, the angles OPN_{amide} are lower than the angles OPN_{amine}.

The differences in the coordination environment of the tin atom and different para substituents on the phenyl ring are not dramatically reflected in the bond lengths within the OPNCO skeleton. The phosphorus–oxygen bond distances are in the range of 1.4907(15)–1.4993(12) Å. The shortest P–N_{amide} bond lengths are observed for **6·CH_3CN** (1.6745(14) and 1.6756(14) Å) and in other complexes this value vary between 1.6813(16) and 1.685(2) Å (Table 6).

Over and above the conformational differences between *all-trans* and *trans–cis* isomers, they form quite distinct patterns in their intermolecular contacts. While the chlorine atoms of *all trans* molecules participate in intermolecular interactions with NH_{amine} groups, the NH_{amine}···Cl hydrogen bonding is completely absent in the *trans–cis* isomers and their NH_{amine} groups are involved in NH···O hydrogen bonds with carbonyl groups (and methoxy groups in **6·CH_3CN**). The same hydrogen bond is also found in **5**, however the structures of **7** and **8** comprise intermolecular C–H···O=C hydrogen bonds instead. Only in **5** and **5·CH_3CN**, without substituent on the phenyl rings, oxygen of carbonyl group and N_{amine} are close enough to form N···O short contact.

4. Conclusions

Some new phosphoramidates and their diorganotin complexes have been synthesized. Irrespective of the solvent and reagent ratio only the hexacoordinate tin complexes were obtained. The structure of ligand **2** and complexes **5**, **5·CH_3CN**, **6·CH_3CN**, **7** and **8** have been determined by X-ray diffraction analysis. The results showed that the solvent of crystallization plays an important role in the formation of *all-trans* or *cis–trans* isomers. So, while crystallization from CH_3CN or toluene produced *all-trans* isomers, crystallization from a mixture of acetonitrile and *n*-hexane yielded essentially the *trans–cis* isomer. The presence of CH_3CN in molecular packing of *trans–cis* isomers might be an important packing factor governing the orientation of the ligands, resulting in different supramolecular structures. In the *all-trans* configurated diorganotins, the Sn–O distance is shorter and the Sn–Cl distance is longer. Comparation between the crystal structure of ligand **2** and its related organotin (**6·CH_3CN**) showed that coordination of the ligand is followed by a number of structural perturbations such as the changes in the bond lengths and bond angles. Some perturbations in the IR and NMR spectra of coordinated ligands were also occurred upon complexation.

Appendix A. Supplementary material

CCDC 709117, 785718, 785720, 785719, 742001 and 785716 contain the supplementary crystallographic data for **2**, **5**, **5·CH_3CN**, **6·CH_3CN**, **7** and **8**, respectively. These data can be obtained free of charge from The Cambridge Crystallographic Data Centre via www.ccdc.cam.ac.uk/data_request/cif. Supplementary data associated with this article can be found, in the online version, at doi:10.1016/j.ica.2010.12.060.

References

[1] L. Pellerito, L. Naggy, Chem. Rev. (Washington, DC, US) 224 (2002) 111–150.
[2] M. Gielen, E.R.T. Tiekink (Eds.), Metallotherapeutic Drugs and Metal-Based Diagnostic Agents, The Use of Metals in Medicine, Wily, New York, 2005.
[3] M. Gielen, A.G. Davies, K.H. Pannell, E.R.T. Tiekink (Eds.), Tin Chemistry: Fundamentals, Frontiers, and Applications, Wily, 2008.
[4] J.L. Lefferts, K.C. Molloy, J.J. Zuckerman, I. Haiduc, C. Guta, D. Ruse, Inorg. Chem. 19 (1980) 1662.
[5] N. Singh, M. Megharaj, W.P. Gates, G.J. Churchman, J. Anderson, R.S. Kookana, R. Naidu, Z. Chen, P.G. Slade, N. Sethunathan, J. Agric. Food Chem. 51 (2003) 2653.
[6] P.H. Terry, A.B. Borkovec, J. Agric. Food Chem. 21 (1973) 500.
[7] E.V. Grigoriev, N.S. Yashina, A.A. Prischenko, M.V. Livantsov, V.S. Petrosyan, W. Massa, K. Harms, S. Wocadlo, L. Pellerito, Appl. Organomet. Chem. 9 (1995) 11.
[8] E.V. Grigorev, N.S. Yashina, A.A. Prischenko, M.V. Livantsov, V.S. Petrosyan, L. Pellerito, M.J. Schafer, Appl.Organomet. Chem. 7 (1993) 353.
[9] M.T. Ben Dhia, M.A.M.K. Sanhoury, L.C. Owono Owono, M.R. Khaddar, Mol. Struct. 892 (2008) 103.
[10] E. Le Coz, J.E. Guerchais, Bull. Soc. Chim. Fr. 1 (1971) 80.
[11] S.J. Ruzicka, A.E. Merbach, Inorg. Chim. Acta 20 (1976) 223.
[12] D. Fàrsaiu, R. Leu, P.J. Ream, J. Chem. Soc., Perkin Trans. 2 (2001) 427.
[13] S.E. Dann, A.R.J. Genge, W. Levason, G. Reid, J. Chem. Soc., Dalton Trans. (1997) 2207.
[14] C.H. Yoder, L.A. Margolis, J.M. Horne, J. Organomet. Chem. 633 (2001) 33.
[15] S.J. Ruzicka, A.E. Merbach, Inorg. Chim. Acta 22 (1977) 191.
[16] D. Tudela, V. Fernàndez, J.D. Tornero, J. Chem. Soc., Dalton Trans. (1985) 1281.
[17] J. Rupp-Bensadon, E.A.C. Lucken, J. Chem. Soc., Dalton Trans. (1983) 495.
[18] S.N. Semenov, E.Yu. Maltsev, I.G. Timokhin, A.A. Drozdov, S.I. Troyanov, Mendeleev Commun. (2005) 205.
[19] N. Pieper, C. Klaus-Mrestani, M. Schürmann, K. Jurkschat, M. Biesemans, I. Verbruggen, J.C. Martins, R. Willem, Organometallics 16 (1997) 1043.
[20] M. Borzechowska, V. Trush, I. Turowska-Tyrk, W. Amirkhanov, J. Legendziewicz, J. Alloys Compd. 341 (2002) 98.
[21] K.O. Znovjyak, O.V. Moroz, V.A. Ovchynnikov, T.Yu. Sliva, S.V. Shishkina, V.M. Amirkhanov, Polyhedron 28 (2009) 3731.
[22] B. Coupez, C. Boehme, G. Wipff, Phys. Chem. Chem. Phys. 4 (2002) 5716.
[23] K. Gholivand, N. Oroujzadeh, F. Afshar, J. Organomet. Chem. 695 (2010) 1383.
[24] K. Gholivand, Z. Shariatinia, J. Organomet. Chem. 691 (2006) 4215.
[25] K. Gholivand, Z. Shariatinia, M. Pourayoubi, Polyhedron 25 (2006) 711.

[26] R.N. Kapoor, P. Guillory, L. Schulte, F. Cervantes-Lee, I. Haiduc, L. Parkanyi, K.H. Pannell, Appl. Organomet. Chem. 19 (2005) 510.
[27] V.G. Kumar Das, Y.C. Keong, C. Wei, P.J. Smith, T.C.W. Mak, J. Chem. Soc., Dalton Trans. (1987) 129.
[28] K. Gholivand, F. Mojahed, Z. Anorg. Allg. Chem. 632 (2006) 1570.
[29] For **2a**: Bruker, SAINTPLUS, v. 6.01, Data Reduction and Correction Program, Bruker AXS, Madison, Wisconsin, USA, 1998.
[30] For **2a**: Bruker, SMART, v.5.059, Bruker Molecular Analysis Research Tool, Bruker AXS, Madison, Wisconsin, USA, 1998.
[31] For **1b**, **1b**·CH_3CN and **4b**: Bruker APEX2 Software Package, Bruker AXS Inc., 5465, East Cheryl Parkway, Madison, WI, 2005, p. 5317.
[32] For **2b**·CH_3CN, **3b**: Bruker, Programs APEX II, version 2.0-1; SAINT, version 7.23A; SADABS, version 2004/1; XPREP, version 2005/2; SHELXTL, version 6.1. Bruker AXS Inc., Madison, WI, USA, 2005.
[33] For **2a**, **3b**: G.M. Sheldrick, SADABS, v. 2.01, Bruker/Siemens Area Detector Absorption Correction Program, Bruker AXS, Madison, Wisconsin, USA, 1998.
[34] For **2a**, **3b**: G.M. Sheldrick, SHELXTL, v. 5.10, Structure Determination Software Suit, Bruker AXS, Madison, WI, USA, 1998.
[35] For **1b**, **1b**·CH_3CN, **4b**: G.M. Sheldrick, SHELXTL, v. 5.10, Structure Determination Software Suit, Bruker AXS, Madison, WI, USA, 1998.
[36] For **2b**·CH_3CN: G.M. Sheldrick, Programs SHELXS97 (Crystal Structure Solution) and SHELXL97 (Crystal Structure Refinement), University of Gottingen, Germany, 1997.
[37] R. Murugavel, R. Pothiraja, S. Shanmugan, N. Singh, R.J. Butcher, J. Organomet. Chem. 692 (2007) 1920.
[38] K. Gholivand, S. Farshadian, Z. Hosseini, K. Khajeh, N. Akbari, Appl. Organomet. Chem. 24 (2010) 700.
[39] M.A.M.K. Sanhoury, M.T. Ben Dhia, M. Nsangou, M.R. Khaddar, Polyhedron 25 (2006) 1373.
[40] J. Holeček, M. Nádvorník, K. Handlíř, A. Lyčka, J. Organomet. Chem. 315 (1986) 299.
[41] D.E.C. Corbridge, Phosphorus an Outline of its Chemistry Biochemistry and Technology, fifth ed., Elsevier, Amsterdam, 1995.
[42] D.G. Gilheany, Chem. Rev. 94 (1994) 1339.
[43] K. Gholivand, A.M. Alizadehgan, F. Mojahed, P. Soleimani, Polyhedron 27 (2008) 1639.
[44] K. Gholivand, Z. Shariatinia, M. Pourayoubi, Z. Anorg. Allg. Chem. 632 (2006) 160.
[45] P.C. Srivastava, S. Bajpai, Sm. Bajpai, R. Kumar, R.J. Butcher, Inorg. Chim. Acta 358 (2005) 227.
[46] J.S. Casas, A. Castineriros, E.G. Martines, A.S. Gonzales, A. Sanches, J. Sordo, Polyhedron 16 (1997) 795.
[47] M. Hill, M.F. Mahon, K.C. Molloy, J. Chem. Soc., Dalton Trans. (1996) 1857.
[48] S. Bhandari, M.F. Mahon, K.C. Molloy, J. Chem. Soc., Dalton Trans. (1999) 1951.
[49] N.W. Alcock, J.F. Sawyer, J. Chem. Soc., Dalton Trans. (1977) 1090.
[50] R. Altmann, K. Jurkschat, M. Schürmann, D. Dakternieks, A. Duthie, Organometallics 17 (1998) 5858.
[51] S.E. Denmark, X. Su, Tetrahedron 55 (1999) 8727.
[52] R. Zhang, G. Tian, C. Ma, J. Organomet. Chem. 690 (2005) 4049.
[53] A.K. Tewari, R. Dubey, ARKIVOC (x) (2009) 283.
[54] K. Gholivand, H.R. Mahzouni, M. Pourayoubi, S. Amiri, Inorg. Chim. Acta 363 (2010) 2318.
[55] F.H. Allen, S.A. Bellard, M.D. Brice, B.A. Cartwright, A. Doubleday, H. Higgs, T. Hummelink, B.G. Hummelink-Peters, O. Kennard, W.D.S. Motherwell, J.R. Rogers, D.G. Watson, Acta Crystallogr., Sect. B 35 (1979) 2331.
[56] A.R. Narga, M. Schuermann, C. Silvestru, J. Organomet. Chem. 623 (2001) 161.
[57] P.J. Smith (Ed.), Chemistry of Tin, second ed., Blackie, London, 1998.
[58] A. Bondi, J. Phys. Chem. 68 (1964) 441.
[59] K. Jurkschat, F. Hesselbarth, M. Dargatz, J. Lehmann, E. Kleinpeter, A. Tzschach, J. Meunier-Piret, J. Organomet. Chem. 388 (1990) 259.